INTERFEROMETRIC IMAGING BY CROSS CORRELATION IN SURFACE SEISMIC PROFILE WITH DOUBLE GREEN'S FUNCTION

CHANG LIU[1,2*], YINGMING QU[1,2], WEIJIE ZHAO[3], SHENGHAN ZENG[4], TINGYU YANG[4] and ZHENCHUN LI[1,2]

[1] School of Geosciences, China University of Petroleum, Qingdao, 266580, P.R. China.
[2] Key Laboratory of Deep Oil and Gas, Qingdao, 266580, P.R. China.
[3] Key Laboratory of Microbial Enhanced Oil Recovery, SINOPEC, Dongying, 257000, P.R. China.
*4 Shengli Branch of Sinopec Petroleum Engineering Geophysics Co., Ltd., Dongying, 257000, China. * 843134767@qq.com*

(Received January 20, 2023; accepted April 25, 2023)

ABSTRACT

Liu, C., Qu, Y.M., Zhao, W.J., Zeng, S.H., Yang, T.Y. and Li, Z.C., 2023. Interferometric imaging by cross-correlation in surface seismic profile with double Green's function. *Journal of Seismic Exploration*, 32: 243-256.

Interferometric imaging aims to revise Green's function for the consequences of acquisition geometry far from the geologic target bodies. That comprises the influences of an irregular acquisition geometry and of complex geological bodies in the overburden such as salt body with very high velocity. The sources can be relocate to positions where receivers are by seismic interferometric technique and vice versa. It is often used in transform data between vertical seismic profile (VSP) and single well profile (SWP), surface seismic profile (SSP) and single well profile. In most cases, no receivers are available at the underground medium, however the propagation of seismic waves in vertical seismic profile can be simulated by finite-difference. By correlating the simulated VSP Green's function with surface seismic data, one can take the acquisition geometry from the surface closer to subsurface datum. The traditional interferometric imaging in surface seismic profile use one kind of VSP Green's function so it only can handle simple model. To overcome this problem, double VSP Green's function interferometric imaging (DGFII) is presented, which can handle complex model. Our numerical examples demonstrate that DGFII works perfectly not only in a homogeneous overburden, but also in a hetergeneous overburden.

KEY WORDS: interferometric imaging, cross-correlation, surface seismic profile, hetergeneous overburden.

0963-0651/23/$5.00

INTRODUCTION

Two-way wave migration is more precise for imaging reflected waves that propagate through sedimentary strata in highly complex media (Biondi et al., 2002), the prerequisites for the method is an accurate migration velocity is used. One example is reverse-time migration (RTM). RTM was presented by Baysal (1983), Loewenthal (1983), McMechan (1983) and Whitmore (1983). Based on the complete solution of the two-way wave equation, RTM has no dip limitation and accounts for wave propagation in any direction (Esmersoy and Oristaglio, 1988). RTM shows great advantages over ray-based method (Beylkin, 1985; Hill 1990; Gray and Bleistein, 2009) and one-way wave equation-based method (Claerbout, 1985) in imaging the complex subsurface structures (Chang and McMechan, 1986, 1990).

Redatuming of seismic data is a classic technique in seismic processing. Its purpose is to simulating the shots and acquiring data both at a new datum (Berryhill, 1979, 1984). Generally located closer to the target in a specific underground area. The main application of the redatuming technique is to correct vertical seismic-profile (VSP) data to accommodate the effects of complex geological structures in irregular surface acquisitions or overburden, such as low-velocity layers or strong lateral variations. The aim is to produce improved single well profile (SWP) data that are easier to process and better illuminate the target (Wapenaar et al., 1992).

In recent years, there has been increasing interest in using interferometry techniques to improve seismic data processing. Seismic interferometry is a subject based on optical physics. It using information contained in seismic data that is not considered in conventional processing (Barrera et al., 2017). Claerbout (1968) was the first to use interferometric techniques. Interferometric redatuming can relocating sources to positions where receivers are and also can relocating receivers to positions where sources are. They both allows to transmit the seismic acquisitions from the surface to subsurface datum.

Xiao and Schuster (2006) implement redatuming in the common-midpoint domain to recover images below salt bodies without velocity model. Schuster and Zhou (2006) summarize correlation based interferometric redatuming methods and compared them with model based techniques. Dong et al. (2007) carry out three-dimesional correlation based interferometric redatuming technique of Luo and Schuster (2004). It achieves RTM of virtual seismic data to improve the imaging results in specific regions. Lu et al., (2008) describe a new strategy for imaging salt flanks which making use of correlation based interferometric redatuming. Van der Neut et al., (2011) presents elastic interferometric redatuming by multidimensional deconvolution, promoting the quality of redatuming results. Curtis and Halliday (2010) put forward a unified representation which combines the correlation type and convolution type. Based on the preliminary work of Curtis and Halliday (2010), Poliannikov (2011) proposes a interferometric redatuming method to recover reflections that are missing in the virtual shot gather due to illumination problems. Ruigrok and

Wapenaar (2012) explore a new approach called global-phase seismic interferometry which takes advantage of the availability of global phases. Tao and Sen (2013) present a new method to recover virtual seismic data from crosscorrelating acquired seismic responses in the plane-wave domain. Nakata et al. (2014) recover direct wave and reflected wave by using seismic interferometry to the recordings of ground motion from regional earthquakes. Aldawood et al. (2015) prove least-squares datuming obviously suppressing artefacts generated by crosscorrelation. Van der Neut et al. (2017) recover virtual reflection wave and transmission wave as if sources and receivers were located at the two datum lines enclosing the target. Zhao and Li (2018) present a interferometric redatuming method based on crosscorrelation in the wavelet domain to suppress the artifacts and noise. Guo and Alkhalifah (2019) carry out a simultaneous inversion for the overburden velocity model and the virtual shot gathers at that datum line. Guo and Alkhalifah (2020) explore a Target-oriented inversion workflow which combines full-waveform inversion and least-squares waveform redatuming. Barrera et al. (2021) present a new method to reduce nonphysical events in interferometric redatuming which only use deconvolution procedure. Liu et al., (2022) combine the matched filter and the supervirtual interferometry to exactly recover dominant surface waves from the field data.

In this paper, we present the theory and application of double VSP Green's functon interferometric imaging, then show several numerical results. Only the velocity model above the datum is needed for the finite-difference solutions in the redatuming step. After redatuming, we can extract the valuable part of the redatumed data to finish follow-up imaging work. We test the DGFII on simple horizontal layered model synthetic data and SEG/EAGE salt model synthetic data. For all these tests, reverse time migration is applied to the original and redatumed data.

Theory of interferometric imaging

The RTM is calculated in the whole model with array of sources and receivers at the surface, the observation system is shown in Fig. 1, and we call this SSP data. The conventional interferometric redatuming only input one kind of VSP green’s function. A bottom-up strategy can reduced computation costs significantly, however it requires the target area is much smaller than the acquisition area (Dong et al., 2009). A two step interferometric redatuming method was presented (Barrera et al., 2017), however it only can handle simple symmetric model. We propose a new interferometric redatuming method input two kinds of VSP green’s function, the observation system is shown in Figs. 2 and 3. Array of shots at the surface and receivers at subsurface datum is demonstrate in Fig. 2. Array of shots at the subsurface datum and receivers at the surface is demonstrate in Fig. 3. Both arrays positioned at subsurface datum is demonstrate in Fig. 4, which also is output of our interferometric redatuming method. Fig. 5 shows the principle of the interferometric redatuming method which move down the acquisition geometry from surface to subsurface datum.

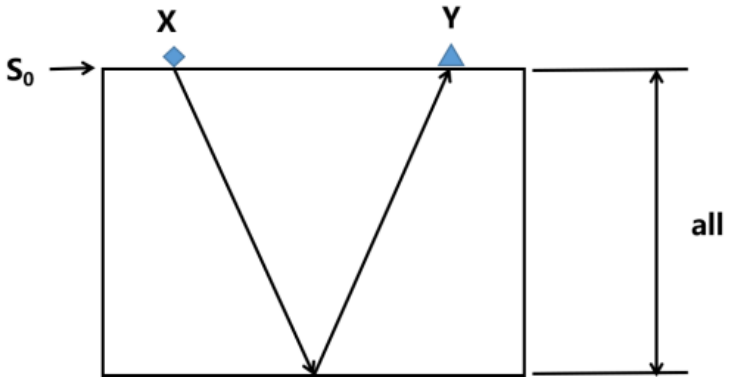

Fig. 1. Sketch of the surface receiver geometry for surface-exciting.

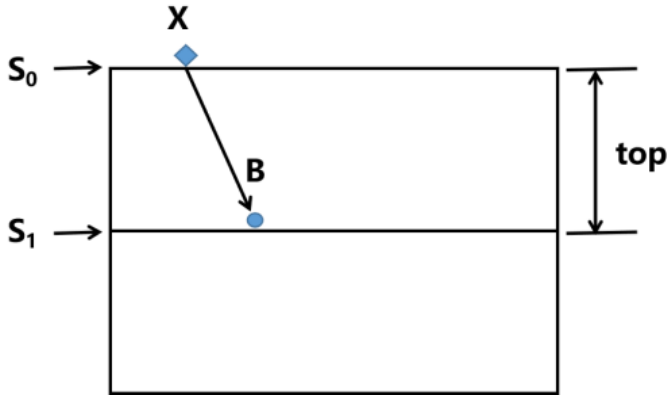

Fig. 2. Sketch of the datum receiver geometry for surface-exciting.

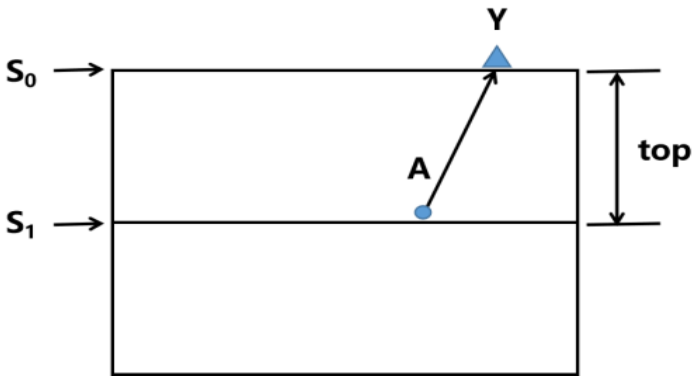

Fig. 3. Sketch of the surface receiver geometry for datum-exciting.

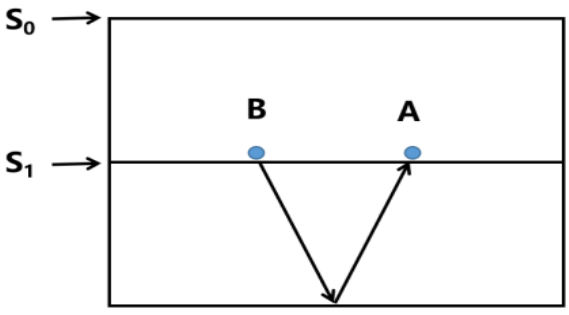

Fig. 4. Sketch of the datum receiver geometry for datum-exciting.

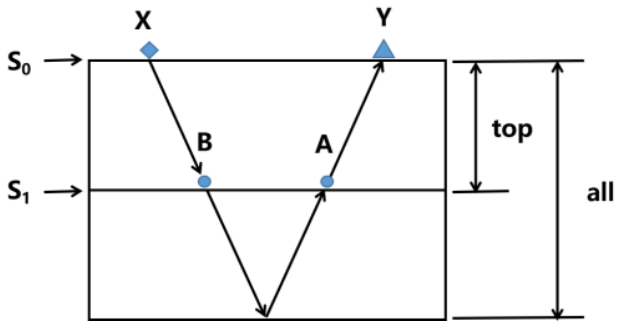

Fig. 5. Sketch of double VSP Green's functon interferometric imaging.

The 2D time-domain acoustic wave equation with constant density with regular-grid discretization can be written as

$$\frac{\partial^2 p}{\partial t^2} = v^2 \nabla^2 p + s \quad , \tag{1}$$

where v is the velocity, s is the source, and p is the pressure field, and t is time.

The acoustic wave equation corresponding to the observation system shown in Fig. 1, Fig. 2 and Fig. 3 can be expressed by the following equation:

$$\frac{\partial^2 p_{(all,S_0)}}{\partial t^2} = v^2 \nabla^2 p_{(all,S_0)} + s_{(all,S_0)} \quad , \tag{2}$$

$$\frac{\partial^2 p_{(top,S_0)}}{\partial t^2} = v^2 \nabla^2 p_{(top,S_0)} + s_{(top,S_0)} \quad , \tag{3}$$

$$\frac{\partial^2 p_{(top,S_1)}}{\partial t^2} = v^2 \nabla^2 p_{(top,S_1)} + s_{(top,S_1)} \quad , \tag{4}$$

where v is the velocity, s is the source, and p is the pressure field, and t is time, *all* represents calculating in the whole model, *top* represents calculating in the model above the datum, S_0 is the model surface, S_1 is the subsurface datum.

In different observation systems, we extract the pressure field at the receivers to form the Green's function:

$$G_{(Y,X)} = p_{(all,S_0;Y,X)} \tag{5}$$

$$G_{(B,X)} = p_{(top,S_0;B,X)} \tag{6}$$

$$G_{(Y,A)} = p_{(top,S_1;Y,A)} \tag{7}$$

where the Green's function $G_{(Y,X)}$ represents the harmonic point-source response of the media, where the source is located at X and the receiver is located at Y, B and A are the receivers on the datum.

Our proposed DGFII method also contains two step but where is no need to resort common-source gathers to common-receiver gathers. In the first step, we call this source-side redatuming, the SSP data would be transform to VSP data which can be written as

$$G_{(Y,B)} = -2i\omega \int_{S_0} \int_{S_1} G_{(B,X)}{}^{*} G_{(Y,X)} dS_0 dS_1 \quad , \tag{8}$$

where the asterisk denotes the complex conjugate, point B X Y can be found in Figs. 1, 2 and 3.

In the second step, we call this receiver-side redatuming, the VSP data would be transform to SWP data which can be written as

$$G_{(A,B)} = -2i\omega \int_{S0} \int_{S1} G_{(Y,A)}{}^{*} G_{(Y,B)} dS_0 dS_1 \quad , \tag{9}$$

where the ω denotes angular frequency, i denotes imaginary unit.

The virtual shot record obtained by seismic interference does not contain the geological information of the overburden medium, and there will be many invalid signal in the shot record end, so the upper part of the shot record can be intercepted manually for post-imaging processing, given as

$$G_{(A,B)}\Big|_{output} = ifft\left(G_{(A,B)}\right)\Big|_{(t_0,t_{\max})} \quad , \tag{10}$$

where the $t_0 = 0$, $t_{\max}$ denotes artificially selected shot record time, *ifft* denotes inverse fast Fourier transform.

The imaging method chosen is RTM, and cross-correlation imaging condition is adopted for imaging, given as

$$I(x,z) = \int_0^T S(x,z,t)R(x,z,t)dt \quad , \tag{11}$$

where $I(x,z)$ is the image, $S(x,z,t)$ is the source wavefeld, $R(x,z,t)$ is the receiver wavefeld.

NUMERICAL EXAMPLES

Two-layer horizontal model

To validate the proposed double VSP Green's functon interferometric imaging method, we conduct an experiment on a Two-layer horizontal model (Fig. 6). The size of the model is set as 2500 $\times$ 2500 and with the grid interval of 5 m. A Ricker wavelet is used as an explosive source at the middle of the surface, with the dominant frequency of 30 Hz. The time sampling increment is 0.5 ms with a total calculation time of 1.0 s. For the SSP geometry in the Two-layer horizontal model, there are 167 shots and 167 receivers at 5-m intervals on the model surface. A typical common-shot gather CSG is shown in Fig. 7a. To calculate one kind of the VSP Green's function (Fig. 2), 167 shots at 5-m intervals are placed along the model surface and 167 receivers at 5-m intervals are located along the horizontal datum line that is 1.5 km beneath the surface (Fig. 7b). To calculate another the VSP Green's function (Fig. 3), 167 shots at 5-m intervals are placed along the horizontal datum line that is 1.5 km beneath the surface and 167 receivers at 5-m intervals are located along the model surface (Fig. 7c). Eqs. (7) and (8) are used to redatum the SSP data so that the redatumed sources and receivers are spread along the pre-selected horizontal datum at a depth of 1.5 km. To check the correctness of the redatumed data, we computed a finite-difference solution to the two-dimensional wave equation for a source at the datum, we call this true CSG. Comparing the redatumed virtual CSG with the true CSG (Figs. 8a and 8b) shows that the major events are accounted correctly, but the curvature of the seismic event is slightly deviated, however it does not affect the imaging effect in the later stage. RTM are calculated using the surface data and the redatumed data. The whole velocity model is used for RTM of SSP shot, although only the part of below the datum of velocity model is needed to migrate the redatumed data. Fig. 9a shows reflector images from RTM of the SSP data after datuming. Fig. 9b shows the RTM image of the original SSP data, note that for the sake of comparison, we only extract the part corresponding to Fig. 9a for display. By comparison, it can be seen that the imaging of Fig. 9a is better. In addition, since we only enter the half upper part of the redatumed data when doing the RTM, it will reduce the calculation time. Computation times for this test are listed in Table 1.

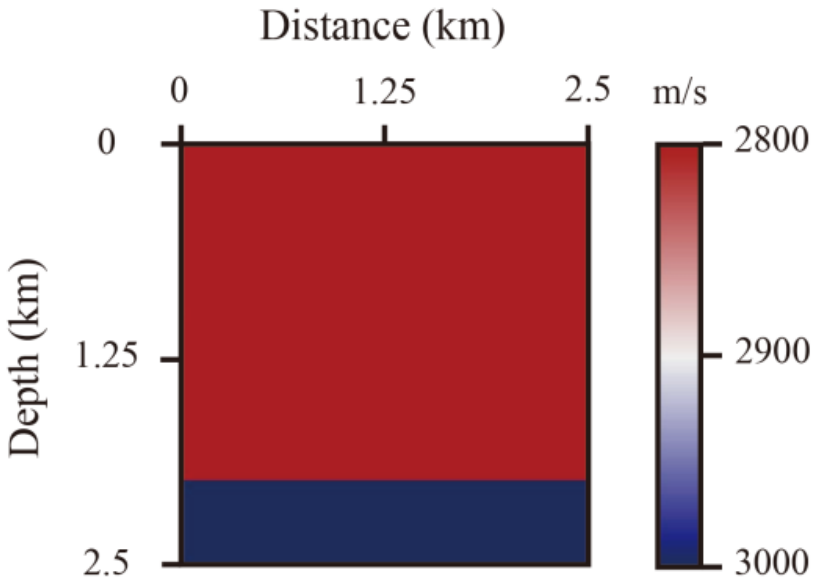

Fig. 6. Two-layer horizontal model.

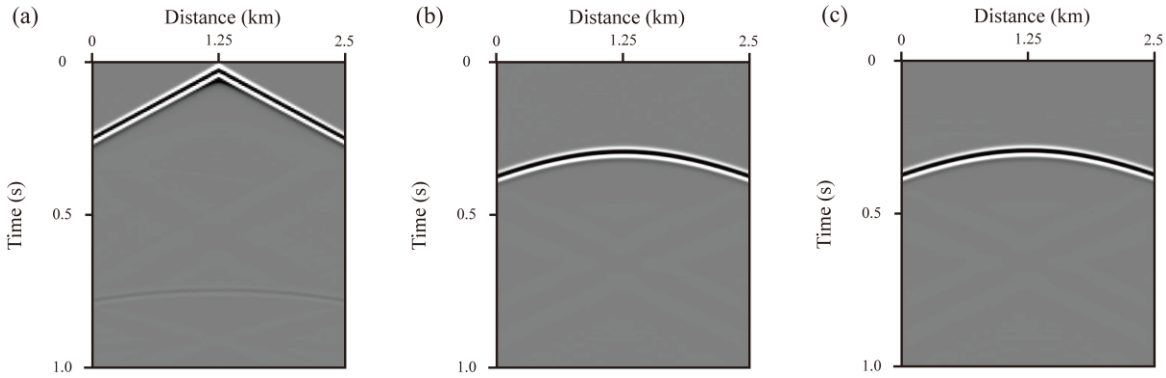

Fig. 7. Redatuming using DGFII with the numerical model of Fig. 6. (a) Original surface data. (b) Modeled VSP Green's of Fig. 2. (c) Modeled VSP Green's of Fig. 3.

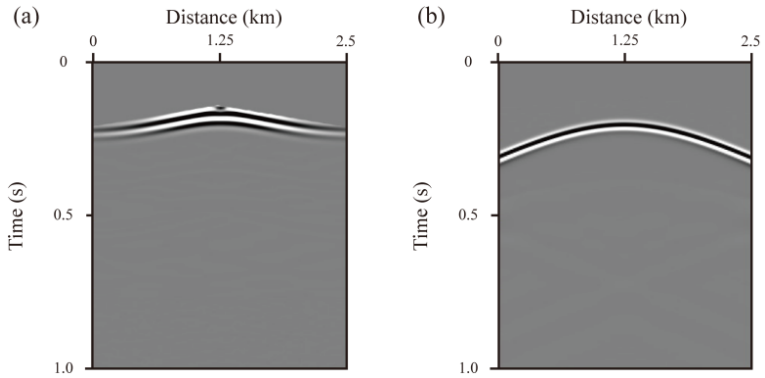

Fig. 8. (a) Redatumed common-shot gather with sources and receivers at a depth of 1.5 km below the surface. (b) A common-shot gather of SSP synthetic seismograms generated from target model depicted in Fig. 6.

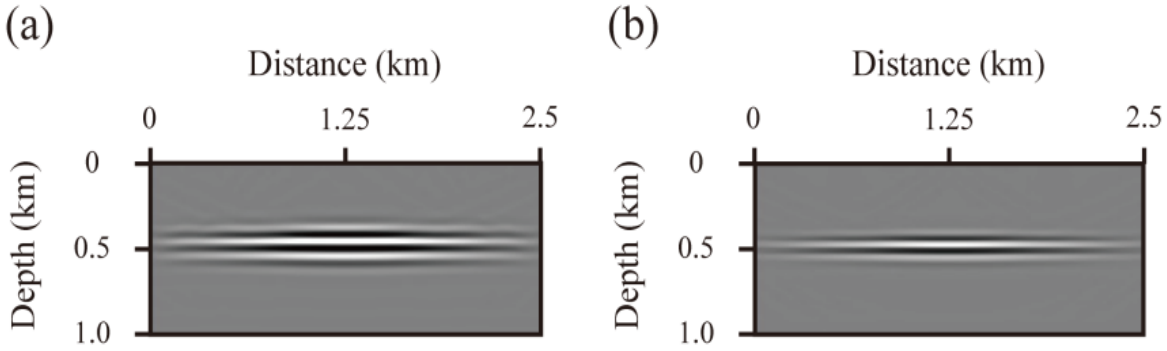

Fig. 9. (a) RTM of redatumed SSP data. (b) The portion of the RTM of original SSP data below the datum depth of 1.5 km.

SEG/EAGE salt model

For the second example, we consider the SEG/EAGE salt model (Fig. 10) to further analyze the capability of the proposed double VSP Green's functon interferometric imaging when imaging a complex subsurface structures. The size of the model is set as 3200 × 850 and with the grid interval of 5 m. A Ricker wavelet is used as an explosive source at the middle of the surface, with the dominant frequency of 30 Hz. The time sampling increment is 0.5 ms with a total calculation time of 2.0 s. For the SSP geometry in the SEG/EAGE salt model, there are 213 shots and 213 receivers at 5-m intervals on the model surface. A typical common-shot gather CSG is shown in Fig. 11a. To calculate one kind of the VSP Green's function (Fig. 2), 213 shots at 5-m intervals are placed along the model surface and 213 receivers at 5-m intervals are located along the horizontal datum line that is 0.55 km beneath the surface (Fig. 11b). To calculate another the VSP Green's function (Fig. 3), 213 shots at 5-m intervals are placed along the horizontal datum line that is 1.5 km beneath the surface and 213 receivers at 5-m intervals are located along the model surface (Fig. 11c). Eqs. (7) and (8) are used to redatum the SSP data so that the redatumed sources and receivers are spread along the artificially selected horizontal datum at a depth of 0.55 km. To check the correctness of the redatumed data, we calculated a finite-difference solution to the two-dimensional wave equation for a source at the datum. Comparing this redatumed virtual CSG with the true CSG (Figs. 12a and 12b) show that the major events are accounted correctly, but some details are still missing, however it does not affect the imaging effect in the later stage. RTM are calculated using the surface data and the redatumed data. The whole velocity model is used for RTM of SSP shot, although only the part of below the datum of velocity model is needed to migrate the redatumed data. Fig. 13a shows reflector images from RTM of the SSP data after datuming. Fig. 13b shows the RTM image of the original SSP data, note that for the sake of comparison, we only extract the part corresponding to Fig. 13a for display. The subsalt portion of the images computed from the redatumed data is of higher quality than the RTM image obtained from the original surface data, especially where the red arrow indicates. In addition, since we

only enter the half upper part of the redatumed data when doing the RTM, it will reduce the computational costs. Computation times for this test are listed in Table 1.

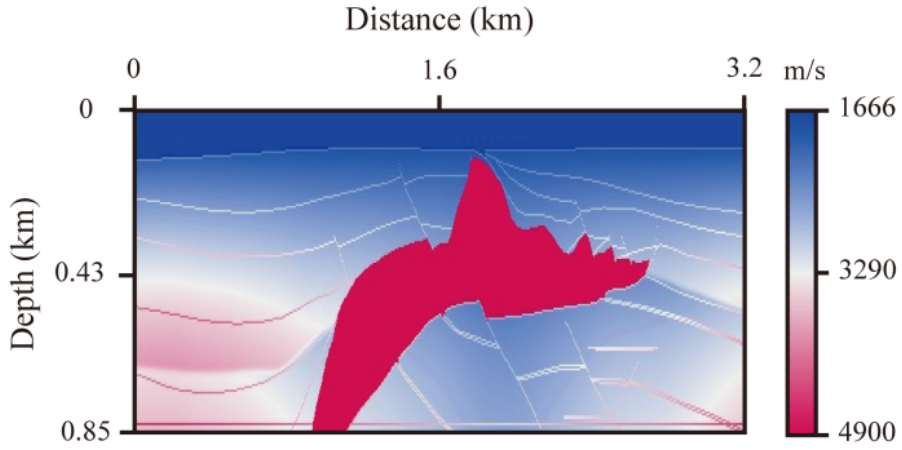

Fig.10. SEG/EAGE salt model.

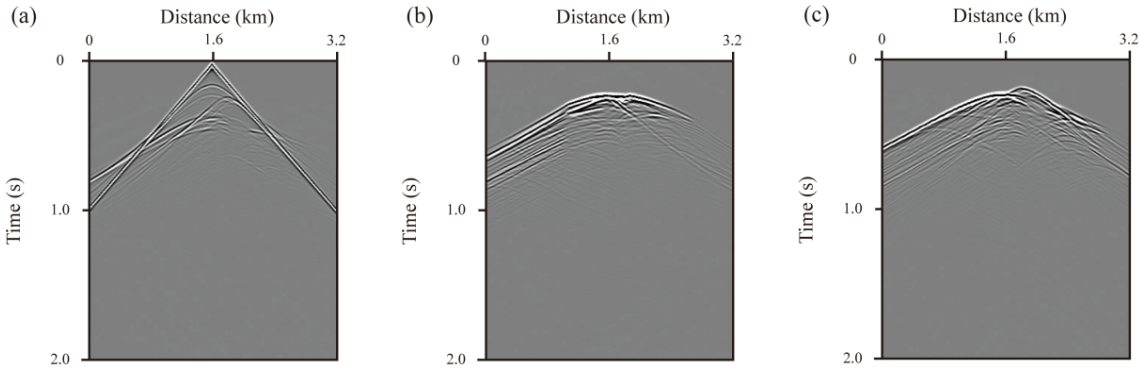

Fig. 11. Redatuming using DGFII with the numerical model of Fig. 10. (a) Original surface data. (b) Modeled VSP Green's of Fig. 2. (c) Modeled VSP Green's of Fig. 3.

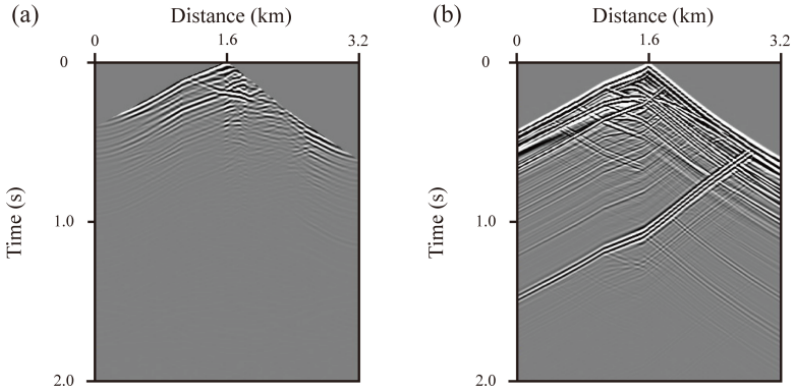

Fig. 12. (a) Redatumed common-shot gather with sources and receivers at a depth of 0.55km below the surface. (b) A common-shot gather of SSP synthetic seismograms generated from target model depicted in Fig. 10.

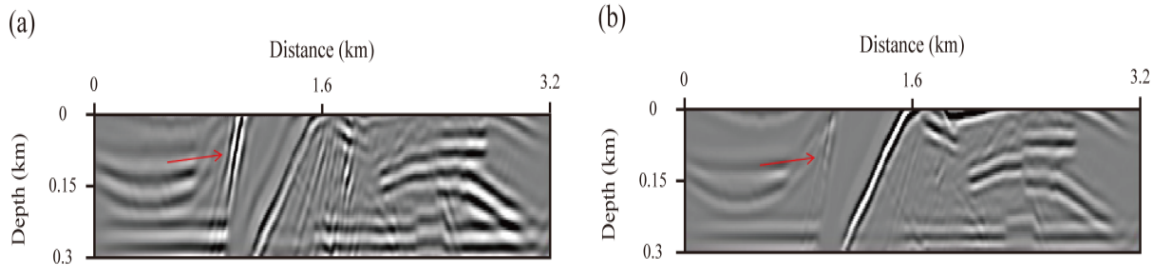

Fig. 13. (a) RTM of redatumed SSP data. (b) The portion of the RTM of original SSP data below the datum depth of 0.55 km.

Table 1. Computation CPU costs for different numerical tests.

Numerical tests	C-RTM	DGFII-RTM
Two-layer horizontal model	1614s	827s
SEG/EAGE salt model	1823s	916s

DISCUSSION

We applied DGFII to the SSP data associated with the Two-layer horizontal model and SEG/EAGE salt model. The redatumed data compared well with the actual shot with sources and receivers located at the new datum. Migration images from redatumed data disclose faults and deep reflectors better than conventional RTM from original SSP data. In the example of SEG/EAGE salt model, the migrated redatumed data exposed the deep structures beneath the salt more evidently, because the redatumed data had been corrected of the defocusing effects of the salt.

A merit of DGFII is that, there is no need to use wavefield extrapolation between the surface and the datum. Only using the crosscorrelation of SSP data at the surface and two kinds of Green's functions. The Green's functions are obtained by forward modeling, which allows a certain scale of smoothness in the input velocity model. In this case, full-volume migration is not necessary, because the virtual shot with sources and receivers located at the new datum can be generated after redatuming. Of particular importance are the redatumed data have simpler seismic events because the distorting effects caused by the overburden are weakened by the redatuming. It is worth mentioning that it is still a challenge to make good use of multiples imaging in redatuming. Our study can be easily extended to three-dimensional media.

CONCLUSIONS

We present a double VSP Green's functon interferometric imaging method, which can generate redatumed data in target areas on a artificially selected underground datum. The recording time of redatumed data is equal to original surface seismic data, however it only contains the information from target area, so we can extract the valuable part of the redatumed data to finish follow-up imaging work. Computation savings are achieved through reducing shot recording time length and longitudinal size of velocity model. This method not only can handle simple symmetrical overburden but also complex overburden, when surface sources and receivers are redatumed to be below it. This is useful for subsalt imaging. Since sources and receivers are closer to the target after redatuming, interferometric imaging has clearer subsalt structure, better resolution and wider illumination. Multiple arrivals that propagate between the surface and the datum are used for imaging below the overburden, the traditional multiple artifact is also enhanced. Several example reverse time migration images from the redatumed data reveal the deep reflectors and salt-dome flanks in the target areas better than images from standard whole model RTM.

ACKNOWLEDGMENTS

This work was supported in part by the Key Laboratory of Deep Oil and Gas, China University of Petroleum (East China); in part by the National Natural Science Foundation of China under Grant 42074133; in part by the Major science and technology cooperation projects of CNPC under Grant ZD2019-183-003.

REFERENCES

Aldawood, A., Hoteit, I., Turkiyyah, G. and Alkhalifah, T., 2015. A study on the effect of least-squares datuming on VSP multiple imaging: a rapidly evolving technology. Extended Abstr., 77th EAGE Conf., Madrid. doi: 10.3997/2214-4609.201413577

Barrera, P., Schleicher, D.F.J. and Brackenhoff, J., 2021. Interferometric redatuming by deconvolution and correlation-based focusing. Geophysics, 86(1), Q1-Q13. doi: 10.1190/geo2019-0208.1

Barrera, P., Schleicher, D.F.J. and van der Neut, J., 2017. Limitations of correlation-based redatuming methods. J. Geophys. Engineer., 14: 1582-1598. doi: 10.1088/1742-2140/aa83cb

Baysal, E., D. D. Kosloff, J. W. C. Sherwood, 1983, Reverse time migration: Geophysics, 48, 1514-1524, doi: 10.1190/1.1441434

Berryhill, J.R., 1979. Wave-equation datuming. Geophysics, 44: 1329-1344. doi: 10.1190/1.1441010

Berryhill, J.R., 1984. Wave equation datuming before stack. Geophysics, 49(11), 2064-2067, doi: 10.1190/1.1441620

Beylkin, G., 1985. Imaging of discontinuities in the inverse scattering problem by inversion of a causal generalized Radon transform: J. Math. Phys, 26: 99-108. doi: 10.1063/1.526755

Biondi, B., Glapp, R.R., Prucha, M. and Sava, P., 2002. 3D prestack waveequation imaging: A rapidly evolving technology. Extended Abstr., 64th EAGE Conf., Florence.

Chang, W. and McMechan, G.A., 1986. Reverse-time migration of offset vertical seismic profiling data using the excitation-time imaging condition. Geophysics, 51: 67-84. doi :10.1190/1.1442041

Chang, W. and McMechan, G.A, 1990. 3D acoustic prestack reverse-time migration. Geophys. Prosp., 38: 737-755. doi: 10.1111/j.1365-2478.1990.tb 01872.x

Claerbout, J.F., 1985. Imaging the Earth's Interior. Blackwell Scientific Publishers, Oxford.

Claerbout, J.F., 1968. Synthesis of a layered medium from its acoustic transmission response. Geophysics, 33: 264-269. doi: 10.1190/1.1439927

Curtis, A. and Halliday, D., 2010. Source-receiver wave field interferometry. Phys. Rev, 81: 046601. doi: 10.1103/PhysRevE.81.046601

Dong, S., Xiao, X., Luo, Y. and Schuster, G., 2007. 3D target-oriented reverse time datuming. Expanded Abstr., 77th Ann. Internat. SEG Mtg., San Antonio, 26: 2442-2445.

Esmersoy, C. and Oristaglio, M., 1988. Reverse-time wave-field extrapolation, imaging, and inversion. Geophysics, 53: 920-931. doi: 10.1190/1.1442529

Gray, S. and Bleistein, N., 2009. True-amplitude Gaussian-beam migration. Geophysics 74(2): S11-S23. doi: 10.1190/1.3052116

Guo, Q. and Alkhalifah, T., 2019. Datum-based waveform inversion using a subsurface-scattering imaging condition. Geophysics, 84(4): S251-S266. doi: 10.1190/GEO2018-0615.1

Guo, Q., and T. Alkhalifah, 2020, Target-oriented waveform redatuming and high-resolution inversion: Role of the overburden: Geophysics, 85(6), R525-R536, doi: 10.1190/GEO2019-0640.1

Hill, N., 1990. Gaussian beam migration. Geophysics, 55: 1416-1428. doi: 10.1190/1.1442788

van der Neut, J., Ravasi, M., Liu, Y. and Vasconcelos, I., 2017. Target-enclosed seismic imaging. Geophysics, 82(6), Q53-Q66. doi: 10.1190/GEO2017-0166.1

Liu, J.H., Draganov, D. and Ghose, R., 2022. Reducing near-surface artifacts from the crossline direction by full-waveform inversion of interferometric surface waves: Geophysics, 87(6): R443-R452. doi: 10.1190/geo2021-0613.1

Loewenthal, D., and I. Mufti, 1983, Reverse time migration in spatial frequency domain: Geophysics, 48, 627-635, doi: 10.1190/1.1441493

Lu, R., Willis, M., Chman, X., Ajo-Franklin, J. and Toksöz, M.N., 2008, Redatuming through a salt canopy and target-oriented salt-flank imaging: Geophysics, 73, S63-71, doi: 10.1190/1.2890704

Luo, Y., and G. Schuster, 2004, Bottom up target-oriented reverse-time datuming: CPS/SEG Int. Geophysical Conf., Expanded Abstracts, 1, 482-485.

McMechan, G. A., 1983, Migration by extrapolation of time-dependent boundary values: Geophysical Prospecting, 31, 413-420, doi: 10.1111/j.1365-2478.1983. 5 tb01060.x

Nakata, N., R. Snieder, and M. Behm, 2014, Body-wave interferometry using regional earthquakes with multidimensional deconvolution after wavefield decomposition at free surface: Geophys. J .Int, 199, 1125-1137, doi: 10.1093/gji/ggu316

Poliannikov, O. V., 2011, Retrieving reflections by source-receiver wavefield interferometry: Geophysics, 76(1), SA1-8, doi: 10.1190/1.3524241

Ruigrok, E., and K. Wapenaar, 2012, Global-phase seismic interferometry unveils P-wave reflectivity below the Himalayas and Tibet: Geophysical research letters, 39, L11303, doi: 10.1029/2012GL051672

Schuster, G. and Zhou, M., 2006. A theoretical overview of model-based and correlation-based redatuming methods. Geophysics, 71(4), SI103-SI10. doi: 10.1190/1.2208967

Tao, Y. and Sen, M.K., 2013. On a plane-wave based crosscorrelation-type seismic interferometry. Geophysics, 78(4), Q35-Q44. doi: 10.1190/GEO2012-0156.1

Van der Neut, J., Thorbecke, J., Mehta, K., Slob, E. and Wapenaar, K., 2011. Controlled-source interferometric redatuming by crosscorrelation and multi-dimensional deconvolution in elastic media. Geophysics, 76(4), SA63-76. doi: 10.1190/1.3580633

Wapenaar, C.P.A., Cox, H.L.H. and Berkhout, A.J., 1992. Elastic redatuming of multicomponent seismic data. Geophys. Prosp., 40: 465-482. doi: 10.1111/j.1365-2478.1992.tb00537.x

Whitmore, N., 1983. Iterative depth migration by backward time propagation. Expanded Abstr., 53rd Ann. Internat. SEG Mtg., Las Vegas: 382-385.

Xiao, X. and Schuster, G., 2006. Redatuming CDP data below salt with VSP Green's function. Expanded Abstr., 76th Ann. Internat. SEG Mtg., New Orleans: 3511-3515.

Zhao, Y. and Li, W.C., 2018. Wavelet-crosscorrelation-based interferometric redatuming in 4D seismic. Geophysics, 83(4): Q37-Q47. doi: 10.1190/GEO2017-0489.1

Dong, S.Q., Luo, Y.,. Xiao, X., Chávez-Pérez, S. and Schuster, G.T., 2009. Fast 3D target-oriented reverse-time datuming. Geophysics, 74(6): WCA141-WCA151. doi: 10.1190/1.3261746